ISSN: 2456-1851

Volume:03, Issue:01 "January-February 2018"

THERMAL BEHAVIOR OF TWO SOLAR COLLECTORS FOR AIR HEATING: ANALYTICAL STUDY

Gabriel Martínez Pereyra[1], Pio Sifuentes Gallardo[1], Angélica Silvestre López Rodríguez[1], Yolanda Córdova Bautista[1], Lizeth Rojas Blanco[1], Erik Ramírez Morales[1], Laura Lorena Díaz Flores[1], Francisco Iván Lizama Tzec[2], Germán Pérez Hernández[1*].

[1]Universidad Juárez Autónoma de Tabasco, Avenida Universidad S/N, Zona de la Cultura, Col. Magisterial, Centro, Villahermosa, Tabasco 86040, México.

[2]Department of Applied Physics, CINVESTAV-IPN, Mérida, Yucatán 97310, Mexico.

*Corresponding author

ABSTRACT

In the present work, we report an analysis of the thermal behavior of two suspended flat plate solar collectors for air heating in forced convection. The objective of this analysis is to determine the improvement in thermal efficiency of suspended flat plate solar collectors by applying a selective coating of nanostructured black nickel to the absorber plate in comparison to suspended corrugated plate solar collectors with matte black commercial coatings. In the first collector both the absorber plate and the lower plate are flat; and the upper side of the absorber plate is painted with a selective nanostructured black nickel coating of low emissivity. In the second collector both the absorber plate and the bottom plate are corrugated and perpendicular to each other; and the upper side of the absorber plate is painted with matte black commercial coating. Incident radiation and ambient temperature were measured in clear days over periods of 15 minutes on May 30, 2017 in Cunduacán Tabasco, Mexico. The thermal efficiency and temperature of the different components of the two collectors were calculated and compared at 15-minute intervals. The results show that efficiency was always greater in the first collector which varies from 73.5 to 75.5 %, and in the second collector from 67.5 to 71.5%, showing a minimum difference between both collectors of 4 % at 13:15 hours and a maximum difference of 6 % at 9:15 15:45 hours. This shows that the selective coating of nanostructured black nickel increases efficiency by reducing radiation losses.

Keywords: Absorbing plate, black nickel, efficiency, selective coating.

NOMENCLATURE

A_c	Collector area (m^2)
C_{pa}	Specific heat of the air (1000 J/kg K)
D_h	Hydraulic diameter (m)
h_{ci}	Heat transfer coefficient by conduction through the lower insulation (W/m^2K)
H_c	Average distance between the absorber plate and the glass cover (m)
$h_{c,uac}$	Convective heat transfer coefficients between the glass cover and the air in the upper channel (W/m^2 K)
$h_{c,lab}$	Convective heat transfer coefficients between air in the lower channel and the bottom plate (W/m^2 K)
$h_{c,uaa}$	Convective heat transfer coefficients between air in the upper channel and the absorber plate (W/m^2 K)
$h_{c,laa}$	Convective heat transfer coefficients between air in the lower channel and the absorber plate (W/m^2 K)
h_{cw}	Convective heat transfer coefficients between glass cover and the wind (W/m^2 K)
H_g	Distance between the absorber plate and lower plate (m)
$h_{r,cs}$	Coefficient of heat transfer by radiation between the glass cover and the sky (W/m^2 K)
$h_{r,ac}$	Coefficient of heat transfer by radiation between the absorber plate and the glass cover (W/m^2 K)
$h_{r,ab}$	Coefficient of heat transfer by radiation between the absorber plate and the lower plate
I	Incident solar radiation on the glass cover (W/m^2)
k_i	Thermal conductivity of the insulation (W/m K)
m_a	Mass flow of air on the upper and lower channel (kg/s)
Nu_{uaa}	Nusselt Number between the absorber plate and the air in the upper channel
Nu_{laa}	Nusselt number between the absorber plate and the air in the lower channel
Nu_{uac}	Nusselt number between the glass cover and the air in the upper channel
Nu_{lab}	Nusselt number between the base plate and the air in the lower channel
Q_{ua}	Useful energy gained in the air of the upper channel (W/m^2)
Q_{la}	Useful energy gained in the air of the lower channel (W/m^2)
Re	Reynolds number
S	Solar radiation absorbed by the absorber plate (W/m^2)
T_{am}	Room temperature (K)

ISSN: 2456-1851

Volume:03, Issue:01 "January-February 2018"

T_c	Temperature in the glass cover (K)
T_s	Temperature of the sky (K)
T_{ua}	Average temperature in the air of the upper channel (K)
T_{la}	Average temperature in the air of the lower channel (K)
T_{uai}	Air inlet temperature in the upper channel (K)
T_{uao}	Air outlet temperature in the upper channel (K)
T_{lai}	Air inlet temperature in the lower channel (K)
T_{lao}	Air outlet temperature in the lower channel (K)
T_a	Temperature in the absorber plate (K)
T_b	Temperature in the lower plate (K)
$\bar{U}_a$	Average speed of the air in the upper and lower channel (m/s)
V_w	Ambient air speed (m/s)
W	Collector width (m)
α_c	Absorptivity of the cover
α_a	Absorptivity of the absorber plate
Δ_i	Average insulation thickness (m)
ϵ_c	Emissivity of glass cover
ϵ_a	Emissivity of the absorber plate
ϵ_b	Emissivity of the lower plate
k_a	Thermal conductivity of the air
σ	Boltzmann Constant (5.67×10^{-8} W/m^2 K)
ρ_a	Air density
τ_c	Transmissivity of the glass cover
μ_a	Dynamic viscosity of the air

1. INTRODUCTION

Solar energy is the most abundant clean and renewable energy source on earth, and the simplest and most efficient way of using it is to convert it into thermal energy using solar collectors [1]. A solar collector is a special type of heat exchanger that transforms radiant solar energy into heat [2] and consists of a surface that absorbs incident solar radiation transmitting it in the form of heat to a working fluid. One of its applications is air heating for processes that do not require a considerably high temperature. Among these processes it can be mentioned solar drying of different agricultural products and heating of rooms. The most important parameter for the evaluation of solar collectors is thermal efficiency which depends on dimensional parameters, air circulation velocity, physical design and prevailing environmental conditions. The thermal efficiency can be increased with the design of the collector configuration by using an absorber plate with fins, a V-corrugated absorber plate, a corrugated absorber plate or a suspended absorber plate of double step, with the incorporation of materials with the capacity to store energy in the absorber plate, and applying a coating to the absorber plate [1, 3, 4, 5, 6, 7, 8, 9, 10]. Sebaii et al. [5] theoretical and experimentally investigated two double-pass solar collectors: flat plate and V-plate collectors; they found that V-plate solar collectors are 11-14% more efficient than flat plate solar collectors.

In solar thermal applications, a coating must have a high absorption capacity but a low emissivity to retain trapped thermal energy. Spectrally selective coatings are a potential alternative in absorber surfaces in low temperature applications as they allow incoming solar radiation to pass through them and block the emissivity of longer wavelength thermal radiation [11]. In this regard W. Gao et al. [9] conducted an analytical and experimental study to investigate the effects of selective coatings on the efficiency of two types of single pass solar collectors with absorber and lower corrugated plates perpendicular to each other and compared it with the efficiency of a collector in which both the absorber plate and the lower plate are flat. They found that without selective coating the corrugated plate collectors are about 10% more efficient than the flat plate collector and between 2 and 6% when selective coating is applied.

In the present work, we report an analysis of the thermal behavior of two suspended plate solar collectors for air heating in forced convection. The aim of this analysis is to determine the thermal efficiency of suspended flat plate solar collectors by applying to the absorber plate a selective coating of nanostructured black nickel developed by F. Tzec et al. [12] in comparison to suspended corrugated plates with matte black commercial coating. In the first collector both the absorber plate and the lower plate are flat; and the upper side of the absorber plate is painted with a selective nanostructured black nickel coating of low emissivity. In the second collector both the absorber plate and the bottom plate are corrugated and perpendicular to each other; and the upper side of the absorber plate is painted with matte black commercial coating. The analysis was based on the studies made by J. Duffie and Beckman [2] which obtained a set of linear equations by means of an energy balance in the cover, the plates and the air. The system of equations was solved by an iterative method using a computer program elaborated in MATLAB considering the radiation as a constant over periods of 15 minutes. Incident radiation and ambient temperature were measured in clear days on May, 2017 in Cunduacán Tabasco, Mexico.

2. THEORETICAL ANALYSIS

The schematic configuration of the proposed solar collectors of suspended plate in forced convection is shown in *Figures. 1 ad 2*. The suspended plate divides the collector in a dual channel that allows air to flow through both sides of the absorber plate increasing the surface area of heat transfer and therefore its efficiency. Both collectors are 1 m long, 0.7 m wide, 0.04 m of spacing in the upper and lower channel, a transparent glass cover 0.003 m thick, an absorbent steel sheet 0.0005 m thick, a polyurethane panel coated with galvanized steel 0.0381 m thick as an

ISSN: 2456-1851

Volume:03, Issue:01 "January-February 2018"

insulation on the sides and bottom of the collector. It is considered that the collectors operate in turbulent regime.

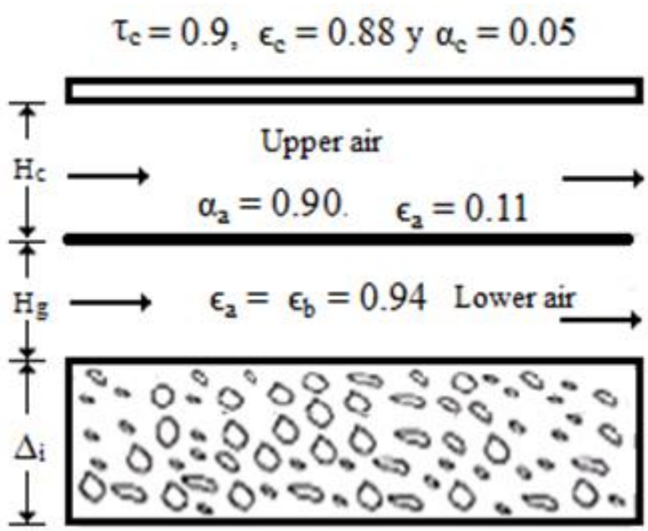

Figure 1: Flat plate solar collector with selective coating

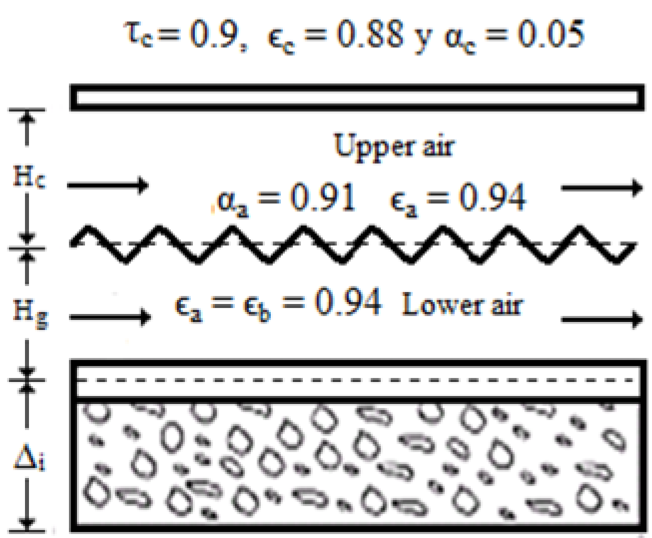

Figure 2: Wavy plate solar collector with black matte commercial coating

ISSN: 2456-1851
Volume:03, Issue:01 "January-February 2018"

Considerations under which the analysis was performed.

- There is an insignificant drop in the temperature of the glass cover, the absorber plate and the bottom plate.
- There is a one-dimensional heat flow through the insulation that is perpendicular to the airflow.
- The sky can be considered as a black body for long wavelength radiation at an equivalent temperature of the sky.
- Losses through the cover are air at room temperature.
- Dust, dirt and shading of the absorption plate are insignificant.
- The thermal inertia of the components of the collector is insignificant.
- The operating temperatures of the components are assumed uniform.
- For a short collector, the air temperature varies linearly in the direction of the flow.
- Air channels are assumed to be free of leaks.
- Thermal losses through the lower insulation of the collector are mainly due to conduction through insulation; those caused by wind and thermal radiation of the insulation are assumed to be negligible.
- The surface of the absorber plate and the glass cover are the same.

The analysis of the solar collector was based on the studies carried out by Duffie and Beckman [2]. Considering that for a short collector the temperatures of the walls surrounding the air are uniform and the air temperatures vary linearly along the collectors [4], the average air temperatures in the upper and lower channel can be expressed as:

$$T_{ua} = (T_{uai} + T_{uao})/2 \qquad \text{(Eq. 1)}$$

$$T_{la} = (T_{lai} + T_{lao})/2 \qquad \text{(Eq. 2)}$$

The equations of the energy balance for the glass cover, the absorber plate and the bottom plate are given by equations, respectively:

$$\alpha_c I + h_{c,uac}(T_{ua} - T_c) + h_{r,ac}(T_a - T_c) = h_{cw}(T_c - T_{am}) + h_{r,cs}(T_c - T_s) \qquad \text{(Eq. 3)}$$

$$\tau_c \alpha_a I = h_{c,uaa}(T_a - T_{ua}) + h_{r,ac}(T_a - T_c) + h_{r,ab}(T_a - T_b) + h_{c,laa}(T_a - T_{la}) \qquad \text{(Eq. 4)}$$

$$h_{r,ab}(T_a - T_b) + h_{c,lab}(T_{la} - T_b) = h_{ci}(T_b - T_{am}) \qquad \text{(Eq. 5)}$$

The equations of the energy balance for the air in the upper and lower channel are, respectively:

$$h_{c,uaa}(T_a - T_{ua}) = \frac{2C_{pa}m_a(T_{ua} - T_{uai})}{A_c} + h_{c,uac}(T_{ua} - T_c) \qquad \text{(Eq. 6)}$$

ISSN: 2456-1851
Volume:03, Issue:01 "January-February 2018"

$$h_{c,laa}(T_a - T_{la}) = \frac{2C_{pa}m_a(T_{la} - T_{lai})}{A_c} + h_{c,lab}(T_{la} - T_b) \quad \text{(Eq. 7)}$$

By rearranging the above equations, we obtain the following equations

$$T_c = \frac{\alpha_c I + h_{c,uac}T_{ua} + h_{r,ac}T_a + h_{cw}T_{am} + h_{r,cs}T_s}{h_{c,uac} + h_{r,ac} + h_{cw} + h_{r,cs}} \quad \text{(Eq. 8)}$$

$$T_a = \frac{\tau_c\alpha_a I + h_{c,uaa}T_{ua} + h_{r,ac}T_c + h_{r,ab}T_b + h_{c,laa}T_{la}}{h_{c,uaa} + h_{r,ac} + h_{r,ab} + h_{c,laa}} \quad \text{(Eq. 9)}$$

$$T_{ua} = \frac{h_{c,uaa}T_a + h_{c,uac}T_c + 2C_{pa}m_aT_{uai}/Ac}{h_{c,uac} + h_{c,uaa} + 2C_{pa}m_a/Ac} \quad \text{(Eq. 10)}$$

$$T_{la} = \frac{h_{c,laa}T_a + h_{c,lab}T_b + 2C_{pa}m_aT_{lai}/Ac}{h_{c,laa} + h_{c,lab} + 2C_{pa}m_a/Ac} \quad \text{(Eq. 11)}$$

$$T_b = \frac{h_{ci}T_{am} + h_{r,ab}T_a + h_{c,lab}T_{la}}{h_{ci} + h_{r,ab} + h_{c,lab}} \quad \text{(Eq. 12)}$$

According to W. Gao et al. [9] the instantaneous efficiency of a solar collector is:

$$\eta = \frac{Q_{ua} + Q_{la}}{IAc} = \frac{c_{pa}m_a}{IAc}[(T_{uao} - T_{uai}) + (T_{lao} - T_{lai})] \quad \text{(Eq. 13)}$$

And total efficiency of the collector according Dote et al. [1] is:

$$\eta_t = \frac{\sum(Q_{ua} + Q_{la})}{A_c \sum I} \quad \text{(Eq. 14)}$$

The following relationships were used [3, 13, 14, 15] to calculate the coefficients of heat transfer by radiation, the heat transfer by convection from the glass cover to wind, the sky temperature and the heat transfer coefficient by conduction through the lower insulation:

$$h_{cw} = 2.8 + 3.3\ _w \quad \text{(Eq. 15)}$$

$$V_w = 1.5m/s \quad \text{(Eq. 16)}$$

$$h_{r,cs} = \sigma\epsilon_c(T_c - T_s)(T_c^2 + T_s^2)\frac{(T_c - T_s)}{(T_c - T_{am})} \quad \text{(Eq. 17)}$$

$$T_s = 0.0552T_{am}^{1.5} \quad \text{(Eq. 18)}$$

$$h_{r,ac} = \frac{\sigma(T_a^2 + T_c^2)(T_a + T_c)}{\frac{1}{\epsilon_a} + \frac{1}{\epsilon_c} - 1} \quad \text{(Eq. 19)}$$

$$h_{r,ab} = \frac{\sigma(T_a^2 + T_b^2)(T_a + T_b)}{\frac{1}{\epsilon_a} + \frac{1}{\epsilon_b} - 1} \quad \text{(Eq. 20)}$$

$$h_{ci} = \frac{k_i}{\Delta_i} \quad \text{(Eq. 21)}$$

The convective heat transfer coefficients were calculated with:

$$h_{c,uaa} = h_{c,uac} = h_{c,laa} = h_{c,lab} = Nu\frac{k}{D_h} \quad \text{(Eq. 22)}$$

where

$$D_h = 2WH_g/(W + H_g) \quad \text{(Eq. 23)}$$

For the first collector, the Nusselt numbers were calculated by the relationship given by [4]:

ISSN: 2456-1851

Volume:03, Issue:01 "January-February 2018"

$$Nu_{uaa} = Nu_{laa} = Nu_{uac} = Nu_{lab} = 0.0158Re^{0.8} \quad \text{(Eq. 24)}$$

And the Reynolds number was calculated with:

$$Re = \frac{2\rho_a \bar{U}_a H_c}{\mu_a} \quad \text{(Eq. 25)}$$

For the second collector, in the case of the cover, the Nusselt numbers were calculated in a similar way as in the first collector. For the absorber and lower plate, the Nusselt numbers were calculated by the relationship given in [9]:

$$Nu_{uaa} = Nu_{laa} = Nu_{lab} = 0.0743Re^{0.76} \quad \text{(Eq. 26)}$$

For this case Reynolds number was calculated with:

$$Re = \frac{\rho_a \bar{U}_a D_h}{\mu_a} \quad \text{(Eq. 27)}$$

For a temperature in the range of 280<T<470 K, the density, thermal conductivity and dynamic viscosity of the air in the upper and lower channels were determined by the following empirical relationships [16]:

$$\rho_a = 3.9147 - 0.016082T + 2.9013x10^{-5}T^2 - 1.9407x10^{-8}T^3 \quad \text{(Eq. 28)}$$

$$k_a = (0.0015215 + 0.097459T - 3.3322x10^{-5}T^2)x10^{-3} \quad \text{(Eq. 29)}$$

$$\mu_a = (1.6157 + 0.06523T - 3.0297x10^{-5}T^2)x10^{-6} \quad \text{(Eq. 30)}$$

Where for the upper channel $T = T_{ua}$ and for the lower channel $T = T_{la}$

3. RESULTS AND DISCUSSION

Since some heat transfer coefficients are functions of temperature, the system of previous equations was solved by an iterative method using a computer program developed in MATLAB language, considering constant the radiation in periods of 15 minutes. The method consisted in assuming initial values for T_c, T_{ua}, T_a, T_{la} and T_b equal to the ambient temperature to calculate the initial heat transfer coefficients, which are then used to estimate the new temperatures, and if all these new temperatures are higher than 0.01% of their respective initially assumed values then these new values will be used for the next iteration, and the process is repeated until all new temperature values obtained are within ± 0.01% of their respective previous values. Considering that according to Ong [4], for a short collector, the temperatures of the walls surrounding the air are uniform and the air temperatures vary linearly along the collector; the collector was divided into 10 short collectors of equal length and width, then the system was solved for the first collector. The next collector was added at the end of the first collector by considering the average initial temperatures of the walls equal to the average temperatures of the walls of the first collector, and the air inlet temperatures of the second collector equal to the air outlet temperatures of the first collector. First collector, and so on,

ISSN: 2456-1851

Volume:03, Issue:01 "January-February 2018"

to consider the 10 collectors. Through this process, the temperatures of the components of the collector were obtained for the first 15 minutes. The temperatures obtained in the first 15 minutes of iteration in the glass cover, the absorber plate, the bottom plate and the ambient temperature measured in the next 15 minutes, were the inlet temperatures for the following 15 minutes and so, successively. It was considered a slope of the collector of 18° (latitude of Cunduacán, Tabasco) and oriented directly towards the south. The solar radiation data at a slope equal to that of the collector and the ambient temperature measured every 15 minutes, corresponding to the day 26 May 2017 from 8:30 to 16:00 hours, are shown in *Figures. 3 and 4.*

The results obtained every 15 minutes by solving the system of equations for both collectors are shown in *Figures. 3, 5-10* for a mass flow of 0.09 kg/s. *Figure 3*, shows the useful heat calculated for the two solar collectors where it is observed that it is slightly larger in the first collector and follows the trend of solar radiation, increasing gradually until reaching a peak value and then decreasing as the solar radiation decreases. The instantaneous efficiency calculated for the different intensities of solar radiation with equation 13 is shown in *Figure 5*. The efficiency for the first collector varied in the range of 73.50 to 75.50 %, and for the second collector in the range of 67.5 to 71.5 % (*Fig. 5*). The efficiency was higher in the first collector, with a minimum difference of 4 % about 13:15 hours and a maximum of 6.0 % about 9:15 and 15:45 between both collectors. The total efficiency calculated with equation (14) was 74.5 % for the first collector, and 70.1 % for the second collector. This shows that the selective coating of nanostructured black nickel increases efficiency by reducing radiation losses. However, the use of a selective coating raises the cost of the collector, a cost-benefit analysis being necessary.

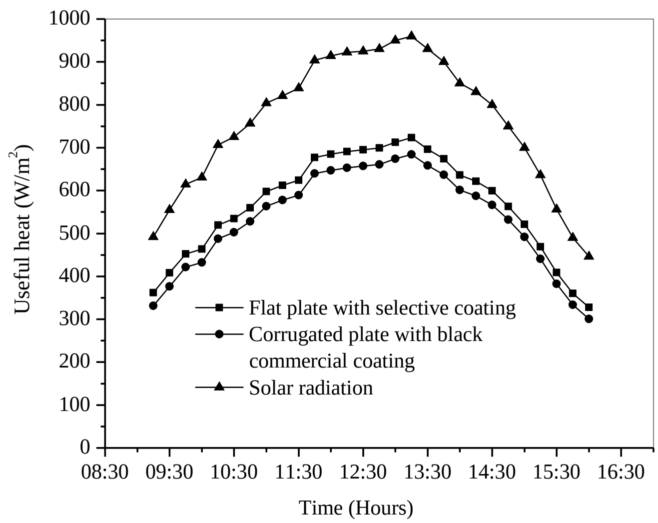

Figure 3: Solar radiation and useful heat variation on May 26th 2017

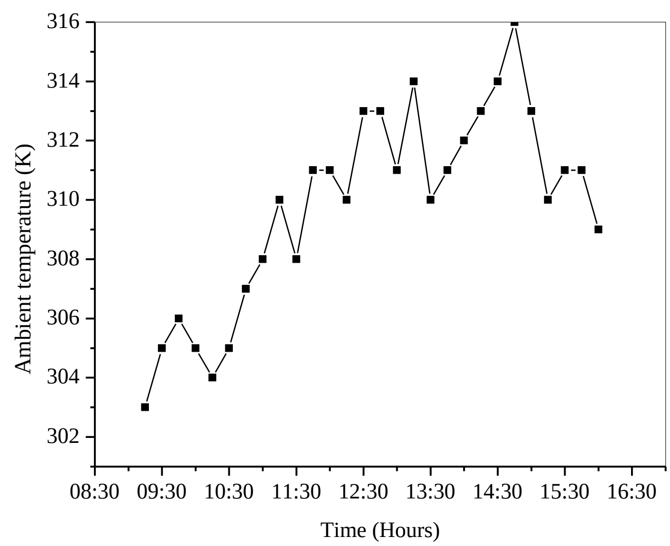

Figure 4: Ambient temperature variation on May 26th 2017

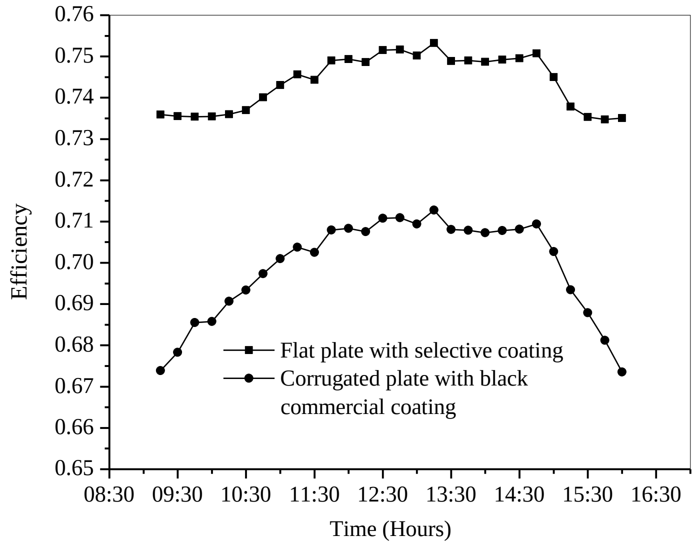

Figure 5: Efficiencies variation

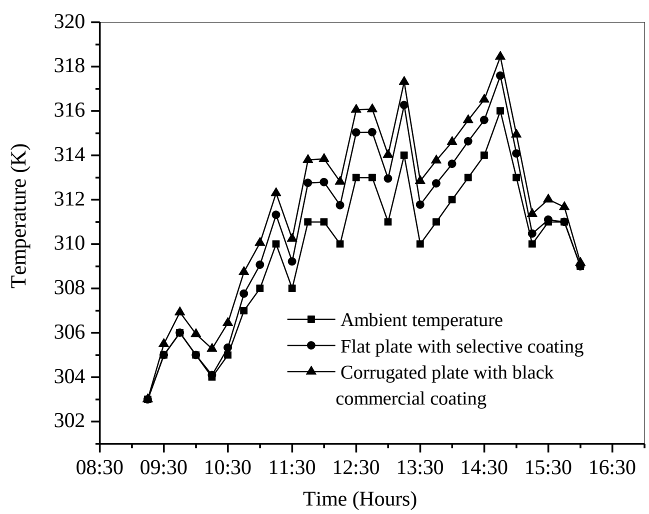

Figure 6: Glass cover temperature variation

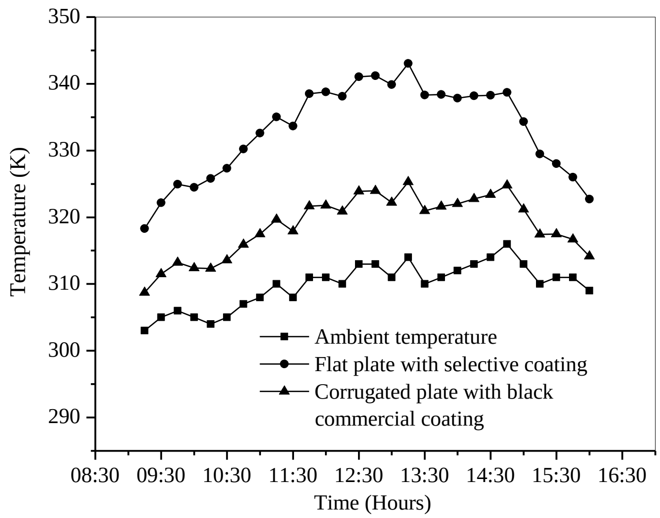

Figure 7: Absorbing plate temperature variation

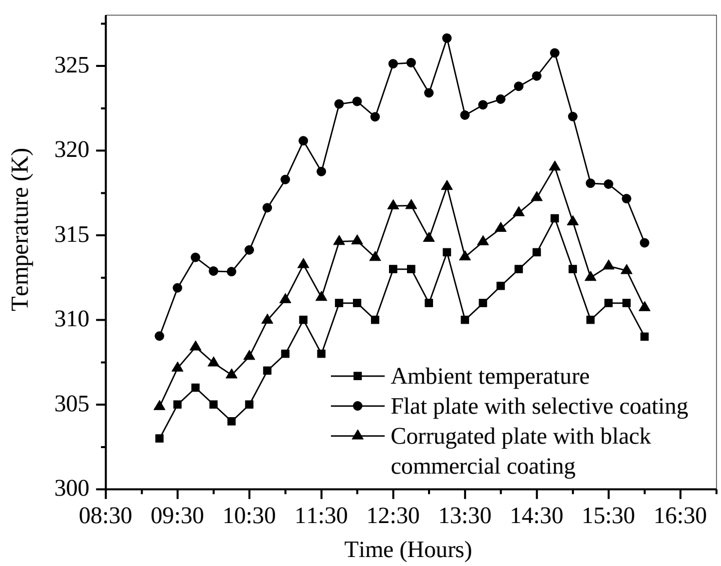

Figure 8: Bottom plate temperature variation

ISSN: 2456-1851
Volume:03, Issue:01 "January-February 2018"

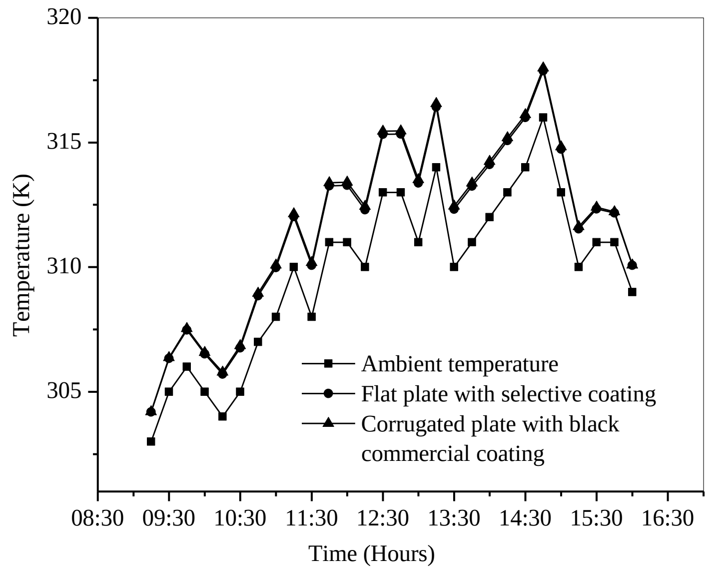

Figure 9: Upper channel air out temperature variation

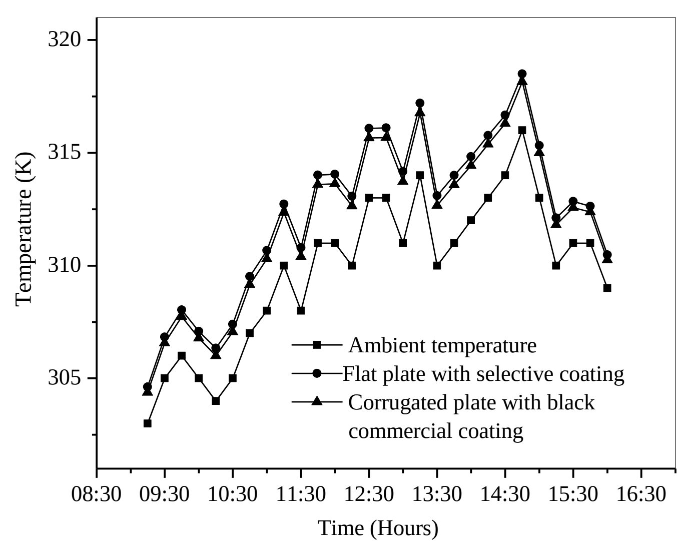

Figure 10: Botton channel air out temperature variation

The temperature variations in the different components of both collectors are shown in *Figures. 6-10*. In the same way as useful heat and efficiency, temperatures follow a behavior similar to solar radiation. In both collectors, the lower temperatures are present in the cover (*Fig. 6*), and the higher temperatures in the absorber plate (*Fig. 7*). This is due to the low absorptivity of the cover and the high absorptivity of the plate absorber. In *Figure 6* it is observed that in the second collector cover the temperatures are higher due to the higher emissivity of the absorber plate, consequently, in the absorber plate of the first collector the temperatures are higher as can be seen in *Figure 7*. In the lower plate (*Fig. 8*), temperatures are higher in the first collector, since the temperatures of the absorber plate in this collector are higher, and in both collectors the emissivity in the lower side of the absorber plate were considered equal causing a greater flow of energy by radiation to the bottom plate in first collector. The variation of the air temperature at the outlet in upper channel in both collectors is shown in *Figure 9* and in the lower channel in *Figure 10*. It can be seen that in both the upper and lower channels, the temperatures are slightly different in both collectors as in the case of the useful heat. This confirm that the low emissivity selective coating on the absorber plate of the first collector increases the efficiency by reducing radiation losses. In the upper channel the temperature is slightly higher for the second collector while in the lower channel the temperature is slightly higher in the first collector, in both cases, according to the calculations by approximately 0.23 K on average.

4. CONCLUSION

By means of an energy balance two solar collectors of different shape in the absorber plate and different coatings were analyzed. The results show a total efficiency of 74.5 % for the first collector and 70.1 % for the second, demonstrating that the selective coating of nanostructured black nickel improves the efficiency of the flat plate solar collector by reducing radiation losses. However, the use of selective coatings increases the cost of the collector, requiring a prior cost-benefit analysis. The variation in temperatures, useful heat and efficiency were in accordance with the trend of the solar radiation, reinforcing the correct execution of the model to evaluate the performance of the analyzed solar collectors.

Acknowledgements

This work was partially supported by the project UJAT-2013-IA_04 UJAT-PFI. To the laboratory national of Nano and Biomaterials (funded by Fomix-Yucatan and Conacyt), CINVESTAV-IPN.

REFERENCES

[1] Dhote, Y., Thombre, S. (2016): Performance Analysis and Parametric Study of a Natural Convection Solar Air Heater With In-built Oil Storage. J. Inst. Eng. India Ser. C 97: 527-537.

[2] Duffie, J., Beckman, W. (2013): Solar Engineering of Thermal Processes. – John Wiley and Sons. Fourth Edition., USA.

[3] Zhao, X., Li, Z. (1991): Numerical and experimental study on free convection in air layers with one surface V corrugated. Proceeding of the annual meeting of the Chinese Society of Solar Energy. 182–192.

[4] Ong, K. S. (1995): Thermal performance of solar air heaters: mathematical model and solution procedure. Solar Energy. 55: 93-109.

[5] EI Sebaii, A., Aboul Enein, S., Ramadan, M., Shalaby, S., Moharram, B. (2011): Investigation of thermal performance of-double pass-flat and v-corrugated plate solar air heaters. Energy. 36: 1076-1086.

[6] EI Sebaii, A., Aboul Enein, S., Ramadan, M., Shalaby, S., Moharram, B. (2011): Thermal performance investigation of double pass-finned plate solar air heater. Applied Energy. 88: 1727-1739.

[7] Koyuncu, T. (2006): Performance of various design of solar air heaters for crop drying applications. Renewable Energy. 31: 1073-1088.

[8] Lin, W., Gao, W., Liu, T. (2006): A parametric study on the thermal performance of cross-corrugated solar air collectors. Applied Thermal Engineering. 26: 1043–1053.

[9] Gao, W., Lin, W., Liu, T., Xia, C. (2007): Analytical and experimental studies on the thermal performance of cross-corrugated and flat-plate solar air heaters. Applied Energy. 84: 425-441.

[10] Yeh, H., Ho, C. (2009): Effect of external recycle on the performances of flat-plate solar air heaters with internal fins attached. Renew Energy. 34: 1340–1347.

[11] Suman, S., Kaleem Khann, M., Manabendra, P. (2015): Performance enhancement of solar collectors-A review. Renewable and Sustainable Energy Reviews. 49: 192-210.

[12] Tzec, F. I. L., Macías, J. D., Gutiérrez, M. A. E., López , A. C. C., Arés, O., de Coss, R., Gil, J. J. A., Oskam, G. (2014): Electrodeposition and characterization of nanostructured black nickel selective absorber coatings for solar–thermal energy conversion. J Mater Sci Mater Electron. 26, 5553–5561.

[13] McAdams, W. (1954): Heat transmission. – McGraw-Hill, New York.

[14] Li, L., Zhao, X. (1991): Studies on the methods of the testing of the thermal performances of solar air collectors. Proceedings of the annual meeting of

the Chinese Society of Solar Energy. 149–155.

[15] Zhai, X., Dai, Y., Wang, R. (2005): Comparison of heating and natural ventilation in a solar house induced by two roof solar collectors. App Therm Eng. 25, 741–57 (2005).

[16] Weast, R. (1970): Handbook of tables for applied engineering science. – Boca Raton: CRC Press.

